Enhancing and sharpening the migration images of gravity field and its gradients

Xiaolei TU[1] and Michael S. Zhdanov[1,2]; [1]CEMI, University of Utah; [2]TechnoImaging*

Summary

Potential field migration represents a rapid technique for imaging the subsurface. However, migration transformation usually produces a smooth and unfocused image of the targets due to the diffusive nature of the potential fields. We introduce a method of the migration image enhancement and sharpening by applying the hybrid focusing stabilizer which combines the edge-preserving smoothing filter with the minimum support functional. The method is based on the model resolution matrix of the migration operator. We also improve the migration image with a novel target-oriented migration method. The developed method of migration image enhancement and sharpening is illustrated by the synthetic model and case studies. The case study involves imaging the gravity gradient data collected in the Nordkapp Basin of the Barents Sea.

Introduction

The measurements of the gravity field and its gradients are extensively used for mapping the subsurface geological structures in mineral, geothermal and hydrocarbon exploration, general geological mapping, and geophysical reconnaissance. During the last decades, several interpretation methods were developed to determine the density distribution in three-dimensional (3D) earth models based on the regularized inversions (e.g., *Li*, 2001; *Zhdanov et al.*, 2004) and a variety of fast imaging techniques (e.g., *Fedi*, 2007; *Beiki*, 2010).

An alternative approach to imaging the potential field data based on an idea of potential field migration was introduced by *Zhdanov* (2002). This approach provided a rapid method of direct transformation of the observed potential field and/or its gradients into 3D density or magnetic susceptibility distributions. Migration can be mathematically described as the action of the adjoint operator on the observed data. This concept has been long developed for seismic wavefields (*Berkhout*, 1980; *Claerbout*, 1985), and was also introduced for electromagnetic (EM) fields (e.g., *Zhdanov et al.*, 1995; *Zhdanov*, 2002). This transformation represents an extrapolation of the field downward and, contrary to the conventional downward continuation, away from the mirror images of the sources. Thus, migration is a stable transformation similar to the conventional upward continuation. However, the migration image of the potential fields without regularization is always diffuse and often poor in spatial resolution.

We have developed a method of the migration image enhancement and sharpening within a general framework of the inverse problem solution. A hybrid focusing stabilizer incorporating the edge-preserving smoothing filter with the minimum support functional is introduced to enhance the sharp boundaries of the anomalous bodies. The method is based on the model resolution matrix of the migration operator, which takes into account the physics and geometry of the survey (*Zhdanov*, 2002; 2015).

Migration of gravity field and its gradients

A. Migration and adjoint operator

Following *Zhdanov* (2002; 2015), the problem of determining the subsurface 3D density distribution from the surface observed gravity and/or gravity gradient data can be solved by migration transformation. The migration of gravity fields is introduced as the action of the adjoint operators, $\mathbf{A}_{\alpha}^{*}$ or $\mathbf{A}_{\alpha\beta}^{*}$, to the observed components of the gravity field, g_{α}, or its gradients, $g_{\alpha\beta}$, respectively:

$$\mathbf{A}_{\alpha}^{*}(g_{\alpha}) = \gamma \iint_{S} \frac{g_{\alpha}(\mathbf{r})}{|\mathbf{r}-\mathbf{r}'|^{3}} K_{\alpha}(\mathbf{r}'-\mathbf{r}) ds', \qquad (1)$$

$$\mathbf{A}_{\alpha\beta}^{*}(g_{\alpha\beta}) = \gamma \iint_{S} \frac{g_{\alpha\beta}(\mathbf{r})}{|\mathbf{r}-\mathbf{r}'|^{3}} K_{\alpha\beta}(\mathbf{r}'-\mathbf{r}) ds', \qquad (2)$$

where γ is the universal gravitational constant; K_{α} and $K_{\alpha\beta}$ are kernels for different components, whose expressions we refer to *Wan and Zhdanov* (2013) and *Zhdanov* (2015). Note that, in the expressions above, the integration is performed over the observation surface, S.

The adjoint operators could also be formulated in Green's functions representation:

$$\mathbf{A}_{\alpha}^{*}(g_{\alpha}) = -\gamma \iint_{S} g_{\alpha}(\mathbf{r}) G_{\alpha}(\mathbf{r}'|\mathbf{r}) ds', \qquad (3)$$

$$\mathbf{A}_{\alpha\beta}^{*}(g_{\alpha\beta}) = \gamma \iint_{S} g_{\alpha\beta}(\mathbf{r}) G_{\alpha\beta}(\mathbf{r}'|\mathbf{r}) ds', \qquad (4)$$

with $G_{\alpha}(\mathbf{r}'|\mathbf{r}) = \frac{K_{\alpha}(\mathbf{r}-\mathbf{r}')}{|\mathbf{r}'-\mathbf{r}|^{3}}$, and $G_{\alpha\beta}(\mathbf{r}'|\mathbf{r}) = \frac{K_{\alpha\beta}(\mathbf{r}-\mathbf{r}')}{|\mathbf{r}'-\mathbf{r}|^{3}}$.

In the derivation of Equation (3) and (4), the gravitational reciprocity principle is employed:

$$G_{\alpha}(\mathbf{r}'|\mathbf{r}) = -G_{\alpha}(\mathbf{r}|\mathbf{r}'), \qquad (5)$$

$$G_{\alpha\beta}(\mathbf{r}'|\mathbf{r}) = G_{\alpha\beta}(\mathbf{r}|\mathbf{r}'). \qquad (6)$$

Thus, the migration of potential field or its gradient is precisely the forward problem of the corresponding adjoint fields and is stable and analytical everywhere in the subsurface. Therefore, migration is a well-posed and stable transform compared with traditional downward

10.1190/segam2019-3214058.1

continuation, which has source-associated singularities in the subsurface and thus ill-posed and unstable.

B. Migration resolution matrix

The adjoint field decays fast with the increase of depth, resulting in fictitious uplift of anomaly positions. A spatial weighting operator is usually introduced to relocate the sources to their correct depth. The migration operator with spatial weights reads:

$$\boldsymbol{\rho}^m = \mathbf{M}(\mathbf{g}) = k(W^*W)\mathbf{A}^*(\mathbf{g}), \tag{7}$$

where W is the diagonal weighting matrix based on the integrated sensitivity (*Zhdanov*, 2002; 2015).

Substituting the forward operator $\mathbf{g} = \mathbf{A}\boldsymbol{\rho}$ into the migration operator, one immediately gets:

$$\boldsymbol{\rho}^m = k(W^*W)\mathbf{A}^*\mathbf{A}\boldsymbol{\rho}. \tag{8}$$

The operator $\mathbf{R} = k(W^*W)\mathbf{A}^*\mathbf{A}$ measures how well the model parameter can be resolved by the migration, and is thus called the migration resolution operator or migration resolution matrix in numerical form:

$$\boldsymbol{\rho}^m = \mathbf{R}\boldsymbol{\rho}. \tag{9}$$

It is apparent from Equation (9) that the migration image is the weighted average of the true model parameters, where the weights are determined by the rows of the resolution matrix. It the true model is a point mass, that is, $\boldsymbol{\rho} = \delta(\mathbf{r} - \mathbf{r}_k)$, the corresponding migration image is $\boldsymbol{\rho}^m = \mathbf{R}^{\cdot k}$, which denotes the kth column of the resolution matrix. Every column represents the migration response of a single point mass anomaly.

C. Target-oriented migration

To take advantage of different components of the gravity and gravity gradiometry data, a joint migration scheme incorporating different field components was introduced by *Wan et al.* (2016):

$$\boldsymbol{\rho}^m = \frac{1}{N_c}\left(\sum \boldsymbol{\rho}_{\alpha}^m + \sum \boldsymbol{\rho}_{\alpha\beta}^m\right), \tag{10}$$

where N_c is the number of field components included; $\boldsymbol{\rho}_{\alpha}^m$ and $\boldsymbol{\rho}_{\alpha\beta}^m$ denote the migration image for different gravity and gravity gradiometry component respectively. An optimal combination of gravitational components for a specific survey should provide the highest sensitivity in the target area and resolve the target to the best. This leads us to the concept of the target-oriented migration.

A joint migration scheme formed by arbitrary combination of the separate migrations:

$$\boldsymbol{\rho}^m = \sum \eta_{\alpha}\boldsymbol{\rho}_{\alpha}^m + \sum \eta_{\alpha\beta}\boldsymbol{\rho}_{\alpha\beta}^m, \tag{11}$$

will result in a joint migration resolution matrix as the combination of separate ones:

$$\mathbf{R}(\boldsymbol{\eta}) = \sum \eta_{\alpha}\mathbf{R}_{\alpha} + \sum \eta_{\alpha\beta}\mathbf{R}_{\alpha\beta}, \tag{12}$$

Our goal is to find an optimal joint resolution matrix which resolves the target model $\boldsymbol{\rho}$ to the best. This can be achieved by minimization of the following functional:

$$\boldsymbol{p}(\boldsymbol{\eta}) = \|\mathbf{R}(\boldsymbol{\eta})\boldsymbol{\rho} - \boldsymbol{\rho}\|^2 \rightarrow \boldsymbol{min}. \tag{13}$$

Equation (13) is a simple linear problem and can be solved easily with least square method.

After finding the optimal coefficients η, one can perform a joint migration based on Equation (11).

Enhancement of migration image

The resolution matrix acts like a blurring matrix that transforms the true image of model parameters into a migration image. The deblurring process involves the inverse of the resolution matrix, which is usually a computationally challenging task. We propose to solve the problem within the framework of the regularized inversion method:

$$p^{\alpha}(\boldsymbol{\rho}) = \|\mathbf{R}\boldsymbol{\rho} - \boldsymbol{\rho}^m\|^2 + \alpha s(\boldsymbol{\rho}) \rightarrow min, \tag{14}$$

where the migration image $\boldsymbol{\rho}^m$ is taken as the observed data; $\boldsymbol{\rho}$ is the true image to be retrieved; $s(\boldsymbol{\rho})$ is a stabilizing functional; α is the regularization parameter that balances the misfit and stabilizing functionals. We solve the above optimization problem with the re-weighted regularized conjugate gradient method (*Zhdanov*, 2002; 2015).

In order to produce the focused images with sharp boundaries we use the minimum support (MS) focusing stabilizer (*Zhdanov*, 2002), which minimizes the volume with nonzero departures from the a priori model, effectively recovering compact bodies. The degree of focusing depends on the focusing parameter, e. However, selection of the optimal focusing parameter is a challenging problem.

We proposed avoiding such problem by incorporating the edge preserving smoothing (EPS) filter in the MS stabilizer (*Luo et al.*, 2002; *AlBinHassan et al.*, 2006). The EPS filter generally produces the same effect as of MS stabilizer, smoothing out the small structures and enhancing the high parameter contrast in the recovered model. We denote the EPS filter by

$$\tilde{\boldsymbol{\rho}} = \mathbf{F}(\boldsymbol{\rho}), \tag{15}$$

where $\boldsymbol{\rho}$ is the input model, and $\boldsymbol{\rho}$ is the filtered model.

10.1190/segam2019-3214058.1

The hybrid focusing stabilizer is introduced as follows:

$$s^h(\boldsymbol{\rho}) = \left(\widetilde{\mathbf{W}}_e(\boldsymbol{\rho} - \boldsymbol{\rho}_{apr}), \widetilde{\mathbf{W}}_e(\boldsymbol{\rho} - \boldsymbol{\rho}_{apr})\right), \quad (16)$$

$$\widetilde{\mathbf{W}}_e^{MS} = \text{diag}[\widetilde{w}_e^{MS}] = diag\left[\frac{1}{\sqrt{(\tilde{\rho} - \rho_{apr})^2 + e^2}}\right], \quad (17)$$

where $\tilde{\rho}$ is a scalar component of the filtered model $\tilde{\boldsymbol{\rho}}$.

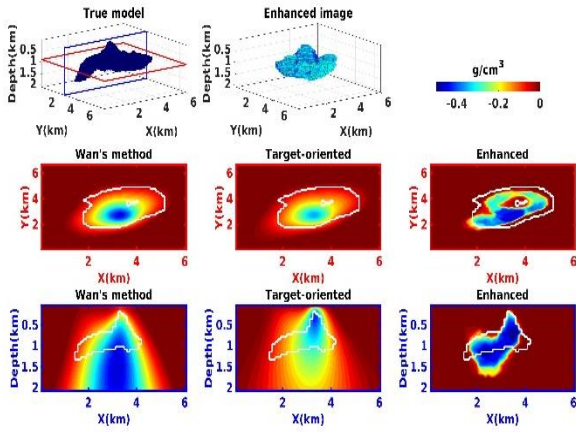

Figure 1: True model and migration images for SEG salt dome. The second row of panels show horizontal sections of migration images; and the third row represents the vertical sections. White solid lines denote the true boundaries of the salt dome. The 3D enhanced image with cutoff value of -0.3g/cm^3 is also shown in the middle panel of the first row.

Model study

We have tested the developed methods with the SEG salt dome model. Following *Zhdanov and Lin* (2017), we consider the anomalous density of the salt dome body to be equal to $-0.5\ \text{g/cm}^3$. The FTG data were computer simulated at 61×61 receiver positions on the sea surface with 120 m intervals for both inline and crossline directions. The data were contaminated with 1% Gaussian noise and migrated with two migration methods. The migration images obtained from both methods are diffusive (Figure 1). The target-oriented migration image has better vertical resolution and is more focused. The target-oriented migration image is further enhanced to promote sharp boundaries. The enhanced image has much sharper edges as demonstrated in Figure 1. The density value and the shape of the salt dome are well retrieved. Especially, details of the salt's top

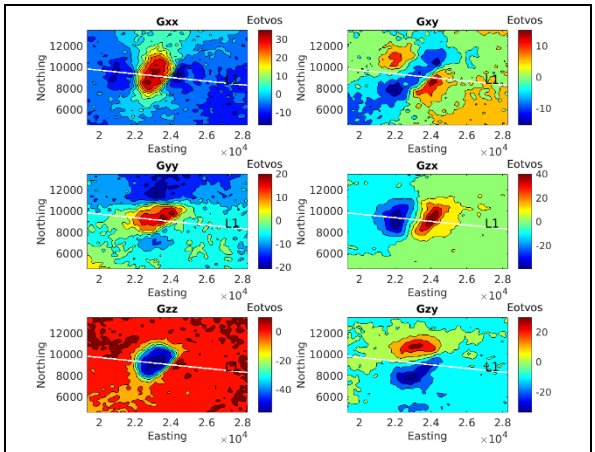

Figure 2: The maps of six independent components of the observed FTG data. White lines denote the known seismic survy line L1.

boundary are completely brought out in the enhanced image, which is challenging to obtain from geopotential data. The bottom boundary is however worse recovered since the sensitivity of the gravity field decreases rapidly with the increase of depth.

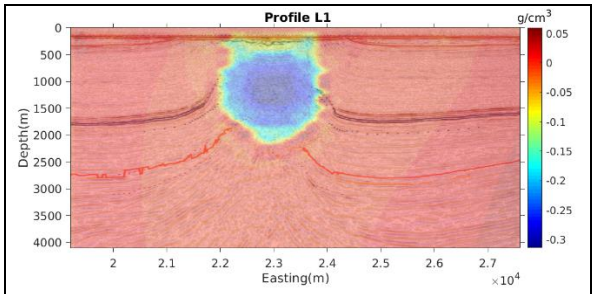

Figure 3: Vertical section of the migration image superimposed on the seismic depth migration.

Case study

To demonstrate the performance of the proposed method, we applied it to the FTG data sets from the Nordkapp Basin (NKB). The NKB is a narrow graben feature in the Western Barents Sea affected by multiple episodes of passive and active diapirism (*Gernigon et al.*, 2011; *Malin*, 2017). Driven by economic interests, lots of efforts have been devoted to understanding the depositional environments and

10.1190/segam2019-3214058.1

salt tectonics in this area (*Koyi et al.*, 1993; *Koyi et al.*, 1995; *Bugge et al.*, 2002; *Gernigon et al.*, 2011; *Malin*, 2017). As a consequence of large acoustic impedance contrast between the salt and surrounding sediments and strong free-surface and internal multiples, it is challenging to picture the complex geometries and extents of salt structures in this area with seismic imaging. Bell Geospace conducted a marine

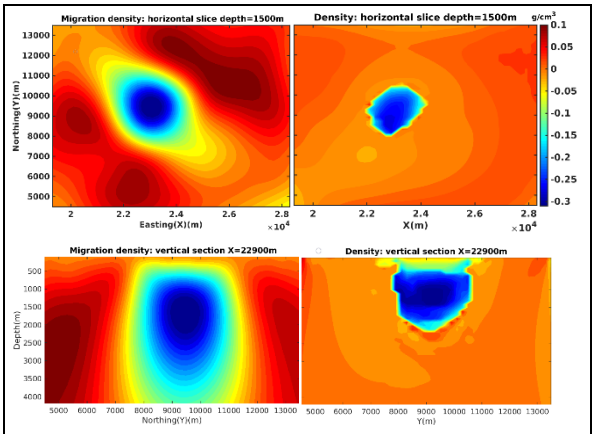

Figure 4: Target-oriented migration and enhanced images. The left panles present the conventional migraion images. The right panels show the enhanced density images.

FTG survey on behalf of StatoilHydro to better delineate the salt geometry (B. Farrelly, personal communication, 2008). A subdomain of 9 km × 9 km where a known salt diapir is located to its center is selected to test our developed algorithms.

There is a seismic survey line (line L1 in Figure 2) runs across the salt diapir; and outlines its horizontal extend very well. However, a large degree of ambiguity about the salt base and pre-salt structures is also presented, as can be seen from the depth migration profile (Figure 3). One should expect that TFG data can provide additional constraints on the salt geometries.

To better understand the salt structures, we first applied the developed target-oriented migration to the six gravity gradiometry components and obtained the migration image, as presented in left column Figure 4. Note that, the migration image shows the location and approximate depth of the salt diapir reasonably well. However, artifacts of positive anomalous density are also presented around the diapir. The diffusive nature of the migration image also poses challenges for interpretation. A further enhancement of the migration density image is performed to improve the resolution of the image.

Figure 4 (right column) presents the horizontal and vertical sections of the enhanced density image. The artifacts are successfully eliminated, and boundaries are well resolved after enhancement. This is also demonstrated in Figure3: the recovered density image shows a good fit with the seismic image along profile L1, both horizontally and vertically. Thus, the enhancement has a strong potential to improve the resolution of migration image especially for geologic targets with sharp density contrast, typical for salt dome structures.

Conclusions

We have developed a target-oriented migration method to improve interpretation of multicomponent gravity and gravity gradiometry data based on the migration algorithms. We have also introduced a method of the migration image enhancement and sharpening based on application of the hybrid focusing stabilizer which combines the edge-preserving smoothing filter with the minimum support functional. The proposed methods have been tested for imaging 3D synthetic density models. The results of our model studies indicate that the target-oriented migration can improve the resolution of migration image compared to conventional method, and it also provides insight in finding the optimal weights for different data components in joint migration of multi-component fields. The migration enhancement method has also been shown having an ability of recovering the shapes and densities of the anomalous bodies at their true depth.

We have applied the developed methods to marine gravity gradiometry data collected in the Nordkapp Basin. The recovered density image shows a good agreement with the known seismic migration images. Thus, the developed methods of image enhancement and sharpening improve the quality of migration images significantly, and make it possible to generate high resolution images with sharp boundaries in an efficient way using migration transformation.

Acknowledgements

The authors acknowledge the support of the University of Utah's Consortium for Electromagnetic Modeling and Inversion (CEMI) and of TechnoImaging.

We are thankful to Dr. B. Farrelly for providing the FTG data.

10.1190/segam2019-3214058.1

REFERENCES

AlBinHassan, N. M., Y. Luo, and M. N. Al-Faraj, 2006, 3D edge-preserving smoothing and applications: Geophysics, **71**, no. 4, P5–P11, doi: https://doi.org/10.1190/1.2213050.

Beiki, M., 2010, Analytic signals of gravity gradient tensor and their application to estimate source locationAnalytic signals of GGT: Geophysics, **75**, no. 6, I59–I74, doi: https://doi.org/10.1190/1.3493639.

Berkhout, A. J., 1980, Seismic migration: Imaging of acoustic energy by wave field extrapolation: Elsevier Scientific Publishing Company.

Bugge, T., G. Elvebakk, S. Fanavoll, G. Mangerud, M. Smelror, H. M. Weiss, J. Gjelberg, S. E. Kristensen, and K. Nilsen, 2002, Shallow stratigraphic drilling applied in hydrocarbon exploration of the Nordkapp Basin, Barents Sea: Journal of Petroleum Science and Engineering, **19**, 13–37, doi: https://doi.org/10.1016/S0264-8172(01)00051-4.

Claerbout, J. F., 1985, Imaging the earth's interior: Blackwell Scientific Publications.

Fedi, M., 2007, DEXP: A fast method to determine the depth and the structural index of potential fields sources: Geophysics, **72**, no. 1, 12JF–Z15. doi: https://doi.org/10.1190/1.2399452.

Gernigon, L., M. Brönner, C. Fichler, L. Løvås, L. Marello, and O. Olesen, 2011, Magnetic expression of salt diaper—related structures in the Nordkapp Basin, western Barents Sea: Geology, **39**, 235–138, doi: https://doi.org/10.1130/G31431.1.

Koyi, H., C. J. Talbot, and B. O. Tørudbakken, 1993, Salt diapirs of the southwest Nordkapp Basin: Analogue modelling: Tectonophysics, **228**, 367–187, doi: https://doi.org/10.1016/0040-1951(93)90339-L.

Koyi, H., C. J. Talbot, and B. O. Torudbakken, 1995, Analogue models of salt diapirs and seismic interpretation in the Nordkapp Basin, Norway: Petroleum Geoscience, **1**, 285–192, doi: https://doi.org/10.1144/petgeo.1.2.185.

Li, Y., 2001, 3-D inversion of gravity gradiometer data: 71st Annual International Meeting, SEG, Expanded Abstracts, 1470–1473, doi: https://doi.org/10.1190/1.1816383.

Luo, Y., M. Marhoon, S. A. Dossary, and M. Alfaraj, 2002, Edge-preserving smoothing and applications: The Leading Edge, **21**, 236–158, doi: https://doi.org/10.1190/1.1452603.

Malin, K. H., 2017, Improved constraint on salt geometry in the southern Nordkapp Basin: Master's thesis: Norwegian University of Science and Technology.

Wan, L., and M. S. Zhdanov, 2013, Iterative migration of gravity and gravity gradiometry data: 83rd Annual International Meeting, SEG, Expanded Abstracts, 1211–1215, doi: https://doi.org/10.1190/segam2013-1036.1.

Wan, L., M. Han, and M. Zhdanov, 2016, Joint iterative migration of surface and borehole gravity gradiometry data: 86th Annual International Meeting, SEG, Expanded Abstracts, 1607–1611, doi: https://doi.org/10.1190/segam2016-13849886.1.

Zhdanov, M. S., 2002, Geophysical inverse theory and regularization problem: Elsevier.

Zhdanov, M. S., 2015, Inverse theory and applications in geophysics, 2nd ed.: Elsevier.

Zhdanov, M. S., and W. Lin, 2017, Adaptive multinary inversion of gravity and gravity gradiometry data: Geophysics, **82**, no. 6, G101–G114, doi: https://doi.org/10.1190/geo2016-0451.1.

Zhdanov, M. S., P. N. Traynin, and O. Portniaguine, 1995, Resistivity imaging by time domain electromagnetic migration (TDEMM): Exploration Geophysics, **26**, 186–194. doi: https://doi.org/10.1071/EG995186.

Zhdanov, M. S., R. Ellis, and S. Mukherjee, 2004, Three dimensional regularized focusing inversion of gravity gradient tensor component data: Geophysics, **69**, 425–937, doi: https://doi.org/10.1190/1.1778236.